Biogeosciences Discuss., 10, 17511–17547, 2013
www.biogeosciences-discuss.net/10/17511/2013/
doi:10.5194/bgd-10-17511-2013


Biogeosciences
Discussions
Open Access



# Climate-mediated spatiotemporal variability in the terrestrial productivity across Europe

**X. Wu[1], M. D. Mahecha[1], M. Reichstein[1], P. Ciais[2], M. Wattenbach[3], F. Babst[4,5], D. Frank[4,6], and C. Zang[7]**

[1]Max Planck Institute for Biogeochemistry, Hans-Knöll-Str. 10, 07745 Jena, Germany
[2]CEA-CNRS-UVSQ, UMR8212-Laboratoire des Sciences du Climat et de l'Environnement (LSCE), Orme des Merisiers, 91191, Gif-Sur-Yvette, France
[3]Helmholtz Centre Potsdam – GFZ German Research Centre For Geosciences, Telegrafenberg, 14473, Potsdam, Germany
[4]Swiss Federal Research Institute WSL, Dendroclimatology, Zürcherstrasse 111, Birmensdorf 8903, Switzerland
[5]Laboratory of Tree-Ring Research, University of Arizona, 1215 E Lowell St, Tucson AZ 85721, USA
[6]Oeschger Centre for Climate Change Research, University of Bern, Bern, Switzerland
[7]Chair of Ecoclimatology, Technische Universität München, Hans-Carl-von-Carlowitz-Platz 2, 85354, Freising, Germany

Received: 2 October 2013 – Accepted: 28 October 2013 – Published: 8 November 2013

Correspondence to: X. Wu (wuxiuchen2000@163.com)

Published by Copernicus Publications on behalf of the European Geosciences Union.

## Abstract

Quantifying the interannual variability (IAV) of the terrestrial productivity and its sensitivity to climate is crucial for improving carbon budget predictions. However, the influence of climate and other mechanisms underlying the spatiotemporal patterns of IAV of productivity are not well understood. In this study we investigated the spatiotemporal patterns of IAV of historical observations of crop yields, tree ring width, remote sensing retrievals of FAPAR and NDVI, and other variables relevant to the terrestrial productivity in Europe in tandem with a set of climate variables. Our results reveal distinct spatial patterns in the IAV of most variables linked to terrestrial productivity. In particular, we find higher IAV in water-limited regions of Europe (Mediterranean and temperate continental Europe) compared to other regions. Our results further indicate that variations in the water balance during active growing season exert a more pronounced and direct effect than variations of temperature on explaining the spatial patterns in IAV of productivity related variables in temperate Europe. We also observe a temporally increasing trend in the IAV of terrestrial productivity and an increasing sensitivity of productivity to water availability in dry regions of Europe, which is likely attributable to the recently increased IAV of water availability in these regions. These findings suggest nonlinear responses of carbon fluxes to climate variability in Europe and that the IAV of terrestrial productivity has become more sensitive and more vulnerable to changes in water availability in the dry regions in Europe. The changing climate sensitivity of terrestrial productivity accompanied by the changing IAV of climate could impact carbon stocks and the net carbon balance of European ecosystems.

## 1 Introduction

One of the largest sources of uncertainties in modelling the future global climate and carbon cycle changes is the response (hereafter called sensitivity) of the terrestrial productivity to climate change and variability. Comprehensive understanding of the sensi-





BGD
10, 17511–17547, 2013

tivity of the interannual variability (IAV) in terrestrial productivity to climate will provide crucial insights as to the future features of the terrestrial carbon balance and its climate feedbacks (Cox et al., 2000; Govindasamy et al., 2005). During the past decades, great efforts were devoted to investigating the IAV in biosphere-atmosphere net carbon exchange and the underlying mechanisms (Kaplan et al., 2012; Moors et al., 2010; Schimel et al., 2001). From these studies it is evident that the terrestrial carbon uptake responds to climate variations and trends on a global scale (Heimann and Reichstein, 2008). The factors controlling terrestrial productivity, its magnitude and spatiotemporal variability are still poorly known (e.g. Keenan et al., 2012) and it is important to quantify and understand them as a pre-requisite for understanding the variability of net carbon fluxes.

It has been demonstrated that several processes including land use changes, natural and/or anthropogenic disturbances, and climate and $CO_2$ variations contribute to variability of productivity (Houghton, 2000; Kaplan et al., 2012; Schimel et al., 2001). Among those processes, land use change and $CO_2$/N fertilization contribute primarily to the changes in terrestrial productivity on long-term time-scales (e.g. decadal, centennial or millennial scales) (Houghton et al., 1999; Jungclaus et al., 2010; Kaplan et al., 2012; Schimel et al., 2001; Zaehle et al., 2010). In contrast, the effects of climate variations are probably the most important driver of IAV in terrestrial productivity on shorter (e.g. seasonal to decadal) time-scales (Barford et al., 2001; Houghton, 2000). This conclusion has been supported by data from diverse ecosystems, including forests (Richardson et al., 2010; Tian et al., 1998; Yuan et al., 2009), grassland (Craine et al., 2012; Flanagan et al., 2002; Jongen et al., 2011; Suyker et al., 2003), cropland (Lei and Yang, 2010), and tundra (Schuur et al., 2009). However, few studies have systematically investigated the sensitivity of terrestrial carbon uptake to interannual variations in climate during past decades, especially on regional to continental scales (Schwalm et al., 2010).

It is particularly notable that the IAV of terrestrial productivity in the well-monitored European sector was found to be very sensitive to short-term climate variability and





BGD
10, 17511–17547, 2013

extreme events (Ciais et al., 2005; Reichstein et al., 2007). A wake-up call in this perspective was the European heatwave in 2003, which resulted in a large reduction in primary production particularly towards the heatwave center of action (i.e. France, Switzerland and western Germany). This effect was large enough to cause a regional negative anomaly in the time series of vegetation greenness index (Ciais et al., 2005). Importantly, the interannual climate variability is projected to increase in the near future over Europe (Schär et al., 2004), particularly in central and eastern Europe according to Seneviratne et al. (2006). Such a regionally different increase in the magnitude of climate IAV could exert poorly understood, yet great effects on productivity, and in turn on regional carbon fluxes. It has also been shown that the sensitivity of IAV of terrestrial productivity to diverse climate variables differs among regions and/or ecosystems (Ciais et al., 2005; Flanagan et al., 2002; Jolly et al., 2005). Despite some progress, the sensitivity of terrestrial productivity to climate IAV of different land use types continues to be a significant source of uncertainty hindering accurate carbon cycle predictions over Europe. For instance, northern high latitudinal vegetation not only showed non-linear responses to climate variability in recent decades, but also showed biome specific characteristics of feedback response (Fang et al., 2005; Jeong et al., 2013). These studies indicate that the sensitivity of the IAV of terrestrial productivity to climate may even depend upon climate state – a characteristic with important implications in the context of dramatic climate change (IPCC, 2012).

Insights as to the past IAV of ecosystem productivity can be obtained from comparing historical multiple proxies, yet it remains insufficient for obtaining a predictive understanding of European terrestrial productivity responses to climate variability. In this study, we therefore address the issue of the sensitivity of terrestrial productivity to inter-annual climate variability in Europe during the past four decades by combining local carbon uptake proxies with regional spatially-extensive carbon uptake observations and associated climate data. Specifically, we aim to (1) identify the spatiotemporal patterns in IAV of terrestrial productivity over Europe from multiple proxies, and (2) assess possibly changing sensitivity of terrestrial productivity to climate IAV over the past decades.

## 2 Data and methods

### 2.1 Datasets

#### 2.1.1 EUROSTAT yield data

We obtained the annual EUROSTAT regional crop yield statistics (according to administrative boundaries at the NUTS 2 level) during 1975–2009 from the European Commission (http://epp.eurostat.ec.europa.eu). This dataset documents all main crop types, such as barley, wheat, grain maize, etc. However, data for most of these crops are scarce. In this study we thus focus on four major kinds of crops with relatively continuous statistics in both the temporal and spatial dimensions: barley, wheat, grain maize and potatoes. In the EUROSTAT database, yield is reported as the amount of dry matter suitable for consumption (Moors et al., 2010).

For each crop, we first examined the length of the available crop yield data for each region and discarded regions with records shorter than ten years. We then filled gaps in the crop yield time series for the remaining regions using a simple linear interpolation method. Only regions with relatively short gaps in crop yield (< 30 % of the total time series) were filled by linear interpolations while regions with longer gaps were further discarded. Our evaluation showed that this gap filling exerts minor effects on crop yield IAV (data not shown). Finally, we rasterized the yield data for each kind of crop from the regions at NUTS2 level to obtain $0.5^\circ \times 0.5^\circ$ gridded yield data matching the resolution of the climate, land cover, and other productivity proxy data (see below). We calculated



Discussion Paper | Discussion Paper | Discussion Paper | Discussion Paper |

BGD

10, 17511–17547, 2013

Climate-mediated variability in the terrestrial productivity

X. Wu et al.

the gridded average crop yield for each crop type, $\bar{y}$, using the following equation:

$$\bar{y} = \left( \sum_{k=1}^{n} A_k C_k \right) / \sum_{k=1}^{n} A_k$$

where $A_k$ is the area fraction of the $k$th region in one grid and $C_k$ is the crop yield of region $k$ obtained from EUROSTAT. In cases where extreme values were present in $C_k$ (i.e. greater or lower than 3 times the standard deviation of the crop yield series for region $k$ during 1975–2009), we assigned the corresponding $A_k$ as 0 to reduce the bias introduced by possibly unrealistic yield records prior to the rasterizing processing. We only retained grid points with cropland fraction $\geq 5\,\%$ based on the International Geosphere Biosphere Programme (IGBP) vegetation classification scheme (Loveland et al., 2000).

### 2.1.2 Tree ring data

Tree-ring width data originated from a large scale database developed by dozens of researchers covering most of Europe (Babst et al., 2013). This tree ring network contains the most abundant tree species in Europe. In this study, we only considered the nine most common and widely distributed tree species in our study region. They are *Abies alba*, *Fagus sylvatica*, *Picea abies*, *Pinus cembra*, *Pinus nigra*, *Pinus sylvestris*, *Quercus petraea* and *Quercus robur*.

Standardized tree ring indices (TRI) were calculated for each site and tree species using standard dendroclimatological procedures (Holmes, 1983; Stokes and Smiley, 1968). We fitted a cubic smoothing spline with a 50 % frequency cutoff response at 32 yr to remove most of the variance related to long-term climatic trends and the biological age-trend (Cook and Peters, 1981). The suitability of each site chronology was evaluated by two criteria: (i) sample depth at site level was greater than five and (ii) the expressed population signal was above 0.85 (Wigley et al., 1984). We then constructed a gridded TRI dataset for each of the 9 tree species with a 0.5° spatial resolution (com-





BGD
10, 17511–17547, 2013

parable to the rasterized crop yield data) by averaging the standardized TRI for each species within pixels. In this study, we only considered the ring width indices between 1975 and 2006 for each tree species and each site to match the others productivity and climate proxies. However, ~ 29–71 % of the chronologies terminate before 1995 for the 9 tree species.

### 2.1.3 NDVI, up-scaled GPP, and FAPAR

Bimonthly Normalized Difference Vegetation Index (NDVI) and Fraction of Absorbed Photosynthetically Active Radiation (FAPAR) data derived from the Advanced Very High Resolution Radiometer (AVHRR) of the National Oceanic and Atmospheric Administration (NOAA) at a spatial resolution of 8 km during 1982–2008 were obtained from the NASA GIMMS (Global Inventory Modeling and Mapping Studies) group. The GIMMS NDVI and FAPAR dataset have been thoroughly corrected for orbit drift, clouds and atmospheric aerosols (Tucker et al., 2005) and have already proved useful to identify long-term changes in vegetation greenness/activities (Forkel et al., 2013; Myneni et al., 1997; Nemani et al., 2003; Zhou et al., 2001). In this study, we resampled the GIMMS NDVI and FAPAR data into monthly data with a spatial resolution of $0.5^\circ \times 0.5^\circ$. The cumulative NDVI and FAPAR during the active growing season is regarded as a good indicator for vegetation activity (e.g. Barichivich et al., 2013). Note that in the comparison with crop yields and TRI time series, the NDVI and FAPAR data were not tiled according to vegetation type, i.e. we compare on each grid cell NDVI and FAPAR averaged across all vegetation types present in that grid cell with other proxies.

Gridded monthly gross primary production (GPP) data over Europe at $0.5^\circ \times 0.5^\circ$ spatial resolution during 1982–2008 period were obtained from Jung et al. (2011). This spatially distributed dataset is constructed by integrating in-situ measurements of FLUXNET data from the La-Thuile-2007 synthesis (www.fluxdata.org) with satellite remote sensing data and meteorological reanalysis (Beer et al., 2010). This observation-based estimation has been demonstrated to add confidence and spatial detail to the global terrestrial GPP (Beer et al., 2010). The gridded GPP product is not independent from FAPAR, given that FAPAR is a key variable in the upscaling of point-wise FLUXNET measurements.

### 2.1.4 Climate data

Monthly temperature (TMP) data from 1975 to 2009 at a $0.5^\circ \times 0.5^\circ$ spatial resolution used in this study were derived from the CRU TS 3.1 dataset (http://www.cru.uea.ac.uk/). The $0.5^\circ \times 0.5^\circ$ gridded water availability index (WAI) data from 1975 to 2009 are estimated based on a simple formula modified from Kleidon and Heimann (1998). Monthly reanalysis data of the number of consecutive frost days (CFD) and the maximum of daily maximum temperature within a month (MMT) for more than 8000 stations over the globe were acquired from the European Climate Assessment (ECA) project (http://www.ecad.eu). We then constructed monthly gridded data for CFD and MMT at a spatial resolution of $0.5^\circ \times 0.5^\circ$ during 1975–2009 by performing a cubic spline spatial interpolation (Tabor and Williams, 2010).

### 2.1.5 Data pre-processing

Long-term trends in the crop yield series during 1975–2009 in different regions of Europe for the same kind of crop are likely caused by technical progress (e.g. breeding), land use policy changes and changes in management practices. The latter could alter the photosynthetic capacity among different crops, even at the same location (Moors et al., 2010). Therefore, we fitted a rigid cubic smoothing spline to each series of crop yield and produced a set of dimensionless indices for different kinds of crops with a mean of one. This was achieved by dividing each crop yield time series by the fitted values, which is analogous to the standard dendrochronological procedures (Babst et al., 2012; Cook and Peters, 1981).

Accordingly, we used the same normalization method to subtract long-term trends in NDVI, GPP, FAPAR and climate data on each grid. The resulting index curves mainly





BGD
10, 17511–17547, 2013

preserve high-frequency variability (e.g. interannual variability) but remove trends and other low-frequency signals in these series (Babst et al., 2012; Cook and Peters, 1997).

The growing season we refer here is the season of active growth, which is vital for vegetation activity and crop production. Although phenology differs between regions in Europe, even for the same kind of crop (Sacks et al., 2010) and tree species (Moser et al., 2010), we attempt to define the growing season in a way that is consistent across Europe. Our approach is supported by observational data showing that the differences in both the planting and the harvest dates for crops are generally within one month between central and southern Europe (Sacks et al., 2010). The active growing season is estimated in this study at monthly, rather than daily resolution which could further smooth the differences in the active growing season intervals between regions in Europe for both crops and tree species. Consequently, we fixed the active growing season as March–June for barley and wheat (hereafter, spring crops) and as March–September for grain maize, potato (hereafter, summer crops) and for all the tree species. However, it should be kept in mind that significant lagged effects from climate during the previous growing (or even dormant) season on radial tree-growth are widely observed (Babst et al., 2013), and may influence the results and interpretation of the tree-ring data in our study (see below).

## 2.2 Methods

### 2.2.1 Spatio-temporal patterns of the IAV for crop yield, tree ring, NDVI, GPP and FAPAR

We evaluated the IAV of detrended crop yield, TRI, and growing season NDVI, GPP and FAPAR (called $NDVI_{gs}$, $GPP_{gs}$, and $FAPAR_{gs}$ hereafter) for each grid by calculating the coefficient of variation (CV) which has been demonstrated as an effective measure of year-to-year variability (Cao et al., 2003; Galloway, 1985). All data sets are compared on an annual basis. The definition of growing season for $NDVI_{gs}$, $GPP_{gs}$ and $FAPAR_{gs}$ is adapted to different kinds of crops and/or TRI (see above). We subsequently quantified spatial patterns of the IAV for different productivity proxies.

Spearman's rank correlation coefficients were used to assess the relationships between the IAV of crop yield, TRI, $NDVI_{gs}$, $GPP_{gs}$ and $FAPAR_{gs}$ for each grid. Correlations of the IAV in these different observations allowed us to investigate possible intrinsic common signals and hence provide insights on the general patterns of IAV of terrestrial productivity across proxies.

The temporal changes in IAV of crop yield, TRI, $NDVI_{gs}$, $GPP_{gs}$ and $FAPAR_{gs}$ in each grid were investigated by calculating the moving CV of the respective time series using a 10 yr window with 1 yr lag during 1975–2009 (if applicable). The choice of the moving window length is a compromise between a large sample size within each window and a sufficient number of windows to evaluate changing IAV. The sign and magnitude of the monotonic trends in moving CVs for the productivity proxies in each grid are estimated by the Theil–Sen slope method, which can provide an accurate estimation of trends in time series with strong autocorrelation (see Yue et al., 2002). Differences in spatiotemporal patterns in the IAV of each productivity proxy among different Köppen–Geiger climate zones are investigated (Kottek et al., 2006). We consider mainly three dominant climate zones in our study including the warm temperate arid zone (Cf, grouping of Cfa, Cfb and Cfc), the warm temperate arid zone (Cs, cluster of Csa and Csb) and the snow humid zone (Df, grouping of Dfa, Dfb and Dfc).

### 2.2.2 Climate relations of IAV of productivity proxies

Response function and general linear model analyses were performed to assess the general relationships between the IAV of different productivity proxies and the corresponding IAV of seasonal climate variables (detrended), including TMP, WAI, CFD and MMT. The response function analysis is a multiple regression technique using principal components of climate data to estimate the values of dependent variables and is widely used in dendroclimatology and dendroecology (Fritts and Wu, 1986; Guiot, 1991). CFD only during spring (March–May) was considered in this analysis because



BGD
10, 17511–17547, 2013
Climate-mediated variability in the terrestrial productivity
X. Wu et al.

frost damages primarily affect vegetation activity and crop yield during this season. The maximum temperature during the active growing season could exert great effects on vegetation activity and crop yield. Therefore, we also introduced growing season MMT into the response function analysis.

### 2.2.3 Changing climate sensitivity of IAV of productivity proxies

For each grid, the interannual sensitivity of the IAV of different productivity proxies to climate variability, $\gamma_{\mathrm{IAV}}$, is assessed based on the least-squares regression formula:

$$\mathrm{CI}_j = \gamma_{\mathrm{IAV}_j} T_j + \varepsilon_j \tag{1}$$

Where $\mathrm{CI}_j$ is the detrended time series of each productivity proxy for period $j$, $T_j$ is the detrended climate variable (either TMP or WAI) for period $j$, and $\varepsilon_j$ is taken as random noise. Strong linkage between $\mathrm{CI}_j$ and $T_j$ yields higher absolute values of $\gamma_{\mathrm{IAVj}}$. In this analysis, only growing season mean temperature and total growing season WAI are taken into account, since these two climate variables are the most important factors determining the IAV of terrestrial productivity (see Sect. 3).

Temporal trends in $\gamma_{\mathrm{IAV}}$ for each grid were evaluated using moving least-squares regressions with a 10 yr sliding window (1 yr lag). The Theil–Sen slope method was again applied to estimate the magnitude and significance of the trends in the changes of $\gamma_{\mathrm{IAV}}$ (Yue et al., 2002).

The distributions of differences in $\gamma_{\mathrm{IAV}}$ of carbon proxies to TMP and WAI between all 10 yr sliding windows in 1982–1995 and those in 1995–2008 (difference matrix of $14 \times 14$ elements for $\gamma_{\mathrm{IAV}}$) are analyzed for different climate zones to further illustrate regional differences in $\gamma_{\mathrm{IAV}}$ trends.





BGD
10, 17511–17547, 2013

## 3 Results

### 3.1 Spatiotemporal patterns of IAV in crop yield, TRI, NDVI, GPP and FAPAR

The IAV of crop yield shows a consistent spatial pattern between the four types of crops, except for potato (Fig. 1). It shows that the IAV of crop yield during 1975–2009 is much larger ($p < 0.05$) in southern Europe (e.g. south of 45° N) than in central Europe, especially for the two spring crops (~ 67 % and ~ 79 % for barley and wheat, respectively) (Fig. 1). Similar patterns are also observed in the IAV of both March–June and March–September summed NDVI, GPP and FAPAR (Supplement Fig. S1). Frequency distribution analyses confirm that the IAV of crop yield is 36 % and 70 % and 30 % and 97 % larger ($p < 0.05$) in drier climate zones (i.e. climate zone Cs) than that in the Cf and Df climate zones for barley and wheat, respectively (Supplement Fig. S2). However, we did not find such patterns in the yield IAV for the two summer crops: maize and potato (Supplement Fig. S2).

Spearman's rank correlation analysis shows a good relationship between the IAV of crop yield and IAV of $NDVI_{gs}$, $GPP_{gs}$, and $FAPAR_{gs}$ during 1982–2008, especially for regions/crops that have a larger IAV in yield records (Figs. 2 and 3). Notably, there is a tendency towards much stronger relationships between IAV of crop yield and IAV of $NDVI_{gs}$, $GPP_{gs}$ and $FAPAR_{gs}$ in the drier regions of Europe (Supplement Fig. S3). In these dry regions, a much higher fraction (~ 45–60 %) of grid cells shows significant ($p < 0.1$) and positive correlations (~ 0.4–0.9) between the IAV of crop yields and IAV of $NDVI_{gs}$, $GPP_{gs}$ and $FAPAR_{gs}$ than other regions (~ 15–30 %) (Fig. 4). In contrast, the TRI dataset did not capture the shared patterns in IAV of spring crop yields, $NDVI_{gs}$, $GPP_{gs}$ and $FAPAR_{gs}$ in any of the Köppen–Geiger climate zones (Fig. 3).

Although there are large differences in the spatial patterns of the linear trends in temporal changes of crop yield IAV, the IAV of detrended crop yields for most of the crops (except for potato) displays a markedly increasing trend in water-limited regions (e.g. the Cs climate zone and some regions in eastern Europe) (Fig. 5). Notably, in these dry regions, the linear trends in CV of accumulative growing season NDVI, GPP and FA-

PAR also show a consistent increase during both March–June and March–September seasons (Supplement Figs. S4 and S5).

### 3.2 Relationships between spatiotemporal IAV of carbon proxies and climate

Response function analysis reveals that the IAV of crop yield in most parts of temperate and Mediterranean Europe responds strongly to the IAV of water availability and negatively to the IAV of temperature, as illustrated by a significant positive (negative) crop yield IAV response coefficient to WAI (TMP) IAV (Fig. 6, Supplement Figs. S6–S8). This conclusion is confirmed by the results of a general linear model, which reveals that the spatial patterns in IAV of productivity proxies generally show significant and positive relationships to the spatial patterns in IAV of WAI in water-limited regions (such as Cs climate zone) and even in some of the temperate humid climate regions (Table 1). Consistent patterns are also observed in the IAV response of March–September accumulated NDVI, GPP, FAPAR to climate (Supplement Figs. S9–S11). The response of different productivity proxies to IAV of CFD did not show coherent spatial patterns (Fig. 6, Supplement Figs. S6–S11). In contrast, all productivity proxies show a coherently significant negative response to the IAV of MMT in most parts of Europe (Fig. 6, Supplement Figs. S6–S11).

### 3.3 Changes in the climate sensitivity of carbon proxies

Despite the great spatial heterogeneity, a generally negative crop yield sensitivty $\gamma_{IAV}$ to mean growing season temperature IAV was obtained during the 1975–2009 period, particularly in eastern and southern Europe (Fig. 7, Supplement Fig. S12). Consistent with this finding, a positive $\gamma_{IAV}$ of IAV of crop yield to total growing season WAI was obtained (Fig. 7, Supplement Fig. S12). Consistent patterns in the general climate sensitivity of productivity proxies such as NDVI, GPP and FAPAR were also observed (Supplement Fig. S13).





BGD
10, 17511–17547, 2013

Notably, there is a pronounced change in $\gamma_{IAV}$ of IAV of crop yield in Europe towards present (Fig. 8). Specifically, there is a generally increasing crop yield $\gamma_{IAV}$ for both TMP and WAI in water-limited regions in Europe (Fig. 8, Supplement Figs. S14 and S15). Increasing climate sensitivity of IAV of accumulative March–September NDVI, GPP and FAPAR to mean March–September temperature and total March–September WAI is also observed in these regions (Supplement Figs. S16–S18). Additionally, there seems to be a generally increasing (but spatially variable) climate sensitivity of IAV of terrestrial productivity to changes in WAI in southern and eastern Europe (Figs. 7 and 8, Supplement Figs. S12–S18). However, we did not observe a consistent pattern in the climate sensitivity of TRI time series from the European tree ring network (data are not shown). Further analysis illustrated that the IAV of productivity in dry-summer temperate and Mediterranean climate zones (i.e. the Cs climate zone) is more sensitive to changing temperature and water availability in the more recent 1995–2008 period than during the1982–1995 period (Fig. 9, Supplement Fig. S19).

## 4 Discussion

### 4.1 Spatiotemporal patterns of IAV of terrestrial productivity and its linkage to climate variations

The majority of productivity proxies consistently indicate that the IAV of terrestrial productivity in Europe is spatially heterogeneous, with much higher IAV in water-limited regions (e.g. southern and eastern Europe) compared to humid oceanic regions (Figs. 1–4, Supplement Figs. S1 and S2). Variations in the water balance (approximated here by the WAI simple index) exert much more important and direct controls (i.e. has a stronger rank correlation) on the spatial patterns in IAV of terrestrial productivity in temperate Europe (i.e. climate zones Cs and Cf) (Table 1) than temperature variations. Water availability is a crucial factor controlling terrestrial productivity at regional scales, especially in arid and semiarid regions (Austin et al., 2004; Huxman et al.,



BGD
10, 17511–17547, 2013

Climate-mediated variability in the terrestrial productivity

X. Wu et al.

2004), whereas the effects of temperature variations on productivity in such regions are mainly by modifying the water availability, evaporative demand and vapour pressure deficit (Williams et al., 2013; Zhao and Running, 2010).

Despite these common patterns, the spatiotemporal patterns of terrestrial productivity IAV across Europe derived from various proxy datasets differ to some extent (Figs. 1 and 3, Supplement Figs. S1 and S2). In particular, the IAV of summer crop yield and TRI are not consistent with the IAV in the other productivity proxies. Summer crops are expected be strongly controlled by intensive human management (e.g. irrigation) and different phenological development stages compared to natural or less intensively managed vegetation. They have also a shorter growing season which makes crop yield sensitive to climate anomalies during short periods, whereas a tree (e.g. a conifer) growing from spring to fall could be negatively affected by climate during one season but could recover during the follow-up part of the growing season. This could partially explain the discrepancies in patterns of IAV between summer crop yield and other proxies. Also, the mismatch between IAV of TRI and some other proxies are most likely explained by both strong carry-over effects of climate on tree growth (Franke et al., 2013), and species-specific growth characteristics (Babst et al., 2013). Also unique to the tree-ring dataset is the heteroscedastic nature of raw tree-ring width measurements whereby the "juvenile" rings tend to be wider with greater year-to-year variability than the outermost rings of older individuals. This behaviour is understood to be largely a by-product of trees placing a more or less constant biomass around an ever increasing circumference, and is accounted for when the age-trend is removed (Cook and Peters, 1997). Furthermore, unlike many of the other proxy datasets, there are fewer tree-ring records in the most recent decade compared with the beginning of the study period (see dataset section), possibly affecting quantification over time.

The IAV of productivity in temperate Europe appears to be more sensitive to variations of extreme temperature conditions (such as MMT), rather than to variations in mean temperature (Table 1). This conclusion is confirmed by increasing evidences and from multi-perspectives (Babst et al., 2012; Ciais et al., 2005; Reichstein et al., 2007;





BGD
10, 17511–17547, 2013

Peng et al., 2013). Importantly, there is an increasing trend in the IAV of productivity proxies (except summer crop yields and TRI) especially in water-limited regions in southern and eastern Europe (Fig. 8, Supplement Figs. S14–S18). The underlying mechanisms for the increasing IAV of productivity in such regions remain unresolved but could at least partially be attributed to increasing variations in climate (Figure S21) and associated changes in vegetation phenology (e.g. Maignan et al., 2008; Zhang et al., 2006). One possible reason for increased IAV of winter crops could be linked to the general average yield increase of these crops over the past decades, i.e. a larger average yield may exhibit a larger risk of being negatively affected by adverse climate conditions a given year. The variations in vegetation carbon uptake and phenology induced by changing climate play a great role in regulating interannual variability of growing season averaged productivity (Wu et al., 2013). Remarkably, there seems to be increased asynchrony between water availability and growing season length in water-limited regions (Austin et al., 2004). Hence, subtle changes in water balance are expected to exert great effects on the productivity in such regions. This finding suggests that the productivity is becoming more vulnerable to the changing climate IAV, especially in water-limited regions. Inference of how a more vulnerable productivity could translate or not into a lesser carbon sinks remain speculative. On the one hand, if the productivity-sink function is concave, a more vulnerable productivity could end up decreasing the carbon sink. On the other hand, for crops that are harvested each year, a more vulnerable productivity could have adverse economical impacts but less effects on the soil carbon balance which is controlled by other factors such as tillage, and non-growing season climate conditions. Furthermore, the region-specific responses of productivity related proxies to climate variations imply that changes in global climate zones and hence vegetation distributions could indirectly alter the relationships between climate variability and carbon balance. This could be expressed e.g. as a northward extension of water limited areas.

Notably, climate variations can only explain 20–40 % of the spatial variance in the IAV of the analysed proxies in most of temperate Europe (Table 1). Some other factors,





BGD
10, 17511–17547, 2013

such as soil water holding capacity, lagged effects, human management (irrigation, fertilization), specific land cover patterns and climate regimes, could contribute significantly to the spatial IAV of terrestrial productivity (Ciais et al., 2010; Gervois et al., 2008). However, the magnitude and individual contribution of these processes to the IAV of carbon cycle remain largely unknown.

## 4.2 Changing sensitivity of productivity proxies to climate variability in Europe

The changing sensitivity of terrestrial productivity variables to climate is expected to have some effects on the carbon balance and associated climate feedbacks (Cox et al., 2000). We observed a coherent significant negative $\gamma_{\mathrm{IAV}}$ of productivity to mean growing season temperature and positive $\gamma_{\mathrm{IAV}}$ to total growing season WAI, in temperate continental and Mediterranean Europe (Fig. 7, Supplement Fig. S12), indicating that the terrestrial productivity in these regions is sensitive to interannual variations of water balance. The change of $\gamma_{\mathrm{IAV}}$ of productivity is ambiguous in western Europe and shows different patterns from other parts of Europe (Fig. 7, Supplement Fig. S12), which is probably linked to the influence of the oceanic climate regime and the lack of a single dominant limitation on productivity (such as water in southern and eastern Europe). Our findings of an increasing $\gamma_{\mathrm{IAV}}$ in southern and temperate eastern Europe are supported by previous studies reporting a divergent response of western European vegetation to climatic fluctuations during the past decade compared with the other parts of Europe (Zhao and Running, 2010). Overall, the IAV of productivity in the water-limited southern and eastern regions in Europe, which are mainly dominated by short-rooted grasslands and croplands, show a higher sensitivity to water availability than in other regions which are less water-limited (Reichstein et al., 2007; Schwalm et al., 2010).

Interestingly, we also observed an increasing sensitivity of productivity to water availability in temperate continental and Mediterranean Europe (Fig. 8, Supplement Figs. S14–18), which may be most likely attributed to the recently increased IAV of water availability in these regions (Fig. S21), due to the non-linear threshold-like response of productivity to water availability and to strong land-atmosphere coupling (Seneviratne et al., 2006). These findings suggest that terrestrial productivity in these regions is becoming more vulnerable to recent changes in water conditions. Notably, simulations predict a considerable enhancement of IAV of European climate, associated with higher risks of heat waves and droughts, in this century (Meehl and Tebaldi, 2004; Schär et al., 2004), suggesting that climate-driven productivity variability will continue to increase over Europe.

Evapotranspiration tends to increase with climate warming likely leading to a more negative water balance in dry regions or to an extension of the total water limited area if precipitation does not increase concurrently (Supplement Fig. S20) (Christensen et al., 2007; Kjellström et al., 2011). The increasing sensitivity of productivity to climate IAV accompanied by an increasing water deficit (Supplement Fig. S20) and changes in plant phenology could lead to a weakening trend in productivity and a weaker carbon sink in this region (Hu et al., 2010; Rivier et al., 2010; Wu et al., 2013). Assimilation is more drought sensitive than respiration and it could further weaken the terrestrial carbon sink in such regions (Schwalm et al., 2010), or even turn them into net carbon sources to the atmosphere.

## 5 Conclusions

The interannual variability of terrestrial productivity in Europe is spatially heterogeneous with much higher IAV in water-limited regions. Despite considerable regional differences, the IAV of productivity and the climate sensitivity showed pronounced temporal changes in Europe during past decades. In water-limited regions in Europe there is an increasing trend in the IAV of productivity and an increasing sensitivity of terrestrial productivity to climate variations, which is at least partly attributable to the increased IAV of climate in these regions. These findings emphasize that the carbon cycle in water-limited regions in Europe is becoming even more vulnerable to changes in water availability. The increasing climate sensitivity of the carbon cycle accompanied by the





BGD
10, 17511–17547, 2013

predicted increase in water deficit could lead to weaker carbon sinks in these regions. Although the terrestrial productivity in Europe responds directly to the changing climate IAV, it could be also regulated to some extent by other factors, such as climate regimes, land use patterns and human footprints. We anticipate that atmospheric inversion and land-surface modelling will be useful to further identify and attribute changes in the climate sensitivity of productivity IAV. Similarly, further development of proxy/historical datasets (e.g. tree ring index, remote sensing observations) should be increasingly regarded as a unique and valuable empirical baseline of carbon cycle processes over the past centuries.

**Supplementary material related to this article is available online at http://www.biogeosciences-discuss.net/10/17511/2013/ bgd-10-17511-2013-supplement.pdf.**

*Acknowledgements.* This work was funded by the CARBO-Extreme project (FP7-ENV-2008-1-226701). The pan-European tree ring network used in this study is a collaborative effort of dozens of researchers. We thank all the participants of the workshop hold in Frankfurt, Germany on 2012 for the CARBO-Extreme project. We also thank Martin Jung in Max Planck Institute for Biogeochemistry and Nicolas Vuichard and Nathalie de Noblet-Ducoudré in Laboratoire des Sciences du Climat et de l'Environnement (LSCE) for their valuable comments. C. Z. acknowledges funding by the European Reseach Council under the European Union's Seventh Framework Programme (FP7/2007-2013)/ERC grant agreement no. [282250].

The service charges for this open access publication
have been covered by the Max Planck Society.





BGD
10, 17511–17547, 2013

## References


Austin, A. T., Yahdjian, L., Stark, J. M., Belnap, J., Porporato, A., Norton, U., Ravetta, D. A., and Schaeffer, S. M.: Water pulses and biogeochemical cycles in arid and semiarid ecosystems, Oecologia, 141, 221–235, 2004.

Babst, F., Carrer, M., Poulter, B., Urbinati, C., Neuwirth, B., and Frank, D: 500 years of regional forest growth variability and links to climatic extreme events in Europe, Environ. Res. Lett., 7, 045705, doi:10.1088/1748-9326/7/4/045705, 2012.

Babst, F., Poulter, B., Trouet, V., Tan, K., Neuwirth, B., Wilson, R., Carrer, M., Grabner, M., Tegel, W., Levanic, T., Panayotov, M., Urbinati, C., Bouriaud, O., Ciais, P., and Frank, D.: Site- and species-specific responses of forest growth to climate across the European continent, Global. Ecol. Biogeogr., 22, 706–717, 2013.

Barford, C. C., Wofsy, S. C., Goulden, M. L., Munger, J. W., Pyle, E. H., Urbanski, S. P., Hutyra, L., Saleska, S. R., Fitzjarrald, D., and Moore, K.: Factors controlling long-and short-term sequestration of atmospheric $CO_2$ in a mid-latitude forest, Science, 294, 1688–1691, 2001.

Barichivich, J., Briffa, K. R., Myneni, R. B., Osborn, T. J., Melvin, T. M., Ciais, P., Piao, S., and Tucker, C.: Large-scale variations in the vegetation growing season and annual cycle of atmospheric $CO_2$ at high northern latitudes from 1950 to 2011, Glob. Change Biol.,19, 3167–3183, 2013.

Beer, C., Reichstein, M., Tomelleri, E., Ciais, P., Jung, M., Carvalhais, N., Rödenbeck, C., Arain, M. A., Baldocchi, D., Bonan, G. B., Bondeau, A., Cescatti, A., Lasslop, G., Lindroth, A., Lomas, M., Luyssaert, S., Margolis, H., Oleson, K. W., Roupsard, O., Veenendaal, E., Viovy, N., Williams, C., Woodward, F. I., and Papale, D.: Terrestrial gross carbon dioxide uptake: global distribution and covariation with climate, Science, 329, 834–838, 2010.

Cao, M., Prince, S. D., Li, K., Tao, B., Small, J., and Shao, X.: Response of terrestrial carbon uptake to climate interannual variability in China, Glob. Change Biol., 9, 536–546, 2003.

Christensen, J. H., Hewitson, B., Busuioc, A., Chen, A., Gao, X., Held, R., Jones, R., Kolli, R. K., Kwon, W. K., Laprise, R., Magana Rueda, V., Mearns, L., Menendez, C. G., Räisänen, J., Rinke, A., Sarr, A., Whetton, P., Arritt, R., Benestad, R., Beniston, M., Bromwich, D., Caya, D., Comiso, J., de Elia, R., and Dethloff, K.: Regional climate projections, in: Climate Change: The Physical Science Basis. Contribution of Working Group I to the Fourth Assessment Report of the Intergovernmental Panel on Climate Change, chapt. 11, University Press, Cambridge, 847–940, 2007, 2007.

Ciais, P., Reichstein, M., Viovy, N., Granier, A., Oée, J., Allard, V., Aubinet, M., Buchmann, N., Bernhofer, C., and Carrara, A.: Europe-wide reduction in primary productivity caused by the heat and drought in 2003: Nature, 437, 529–533, 2005.
Ciais, P., Wattenbach, M., Vuichard, N., Smith, P., Piao, S., Don, A., Luyssaert, S., Janssens, I., Bondeau, A., and Dechow, R.: The European carbon balance. Part 2: Croplands, Glob. Change Biol., 16, 1409–1428, 2010.
Cook, E. R. and Peters, K.: The smoothing spline: a new approach to standardizing forest interior tree-ring width series for dendroclimatic studies, Tree-Ring Bullet., 41, 45–53, 1981.
Cook, E. R. and Peters, K.: Calculating unbiased tree-ring indices for the study of climatic and environmental change, Holocene, 7, 361–370, 1997.
Cox, P. M., Betts, R. A., Jones, C. D., Spall, S. A., and Totterdell, I. J.: Acceleration of global warming due to carbon-cycle feedbacks in a coupled climate model, Nature, 408, 184–187, 2000.
Craine, J. M., Nippert, J. B., Elmore, A. J., Skibbe, A. M., Hutchinson, S. L., and Brunsell, N. A.: Timing of climate variability and grassland productivity, P. Natl. Acad. Sci. USA, 109, 3401–3405, 2012.
Dahlke, C., Loew, A., and Reick, C.: Robust identification of global greening phase patterns from remote sensing vegetation products, J. Climate, 25, 8289–8307, 2012.
Fang, J. Y., Piao, S. L., Zhou, L. M., He, J. S., Wei, F. Y., Myneni, R. B., Tucker, C. J., and Tan, K.: Precipitation patterns alter growth of temperate vegetation, Geophys. Res. Lett., 32, L21411, doi:10.1029/2005gl024231, 2005.
Flanagan, L. B., Wever, L. A., and Carlson, P. J.: Seasonal and interannual variation in carbon dioxide exchange and carbon balance in a northern temperate grassland, Glob. Change Biol., 8, 599–615, 2002.
Forkel, M., Carvalhais, N., Verbesselt, J., Mahecha, M. D., Neigh, C. S. R., and Reichstein, M.: Trend change detection in NDVI time series: effects of inter-annual variability and methodology, Remote Sens., 5, 2113–2144, 2013.
Franke, J., Frank, D., Raible, C. C., Esper, J., and Bronnimann, S.: Spectral biases in tree-ring climate proxies, Nat. Clim. Change, 3, 360–364, 2013.
Fritts, H. C. and Wu, X.: A comparison between response-function analysis and other regression techniques, Tree-Ring Bullet., 46, 31–46, 1986.
Galloway, P. R.: Annual variations in deaths by age, deaths by cause, prices, and weather in London 1670 to 1830, Population Studies, 39, 487–505, 1985.





BGD
10, 17511–17547, 2013

Gervois, S., Ciais, P., De Noblet-Ducoudré, N., Brisson, N., Vuichard, N., and Viovy, N.: Carbon and water balance of European croplands throughout the 20th century, Global Biogeochem. Cy., 22, GB2022, doi:10.1029/2007GB003018, 2008.

Govindasamy, B., Thompson, S., Mirin, A., Wickett, M., Caldeira, K., and Delire, C.: Increase of carbon cycle feedback with climate sensitivity: results from a coupled climate and carbon cycle model, Tellus B, 57, 153–163, 2005.

Guiot, J.: The bootstrapped response function, Tree-Ring Bullet, 51, 39–41, 1991.

Heimann, M. and Reichstein, M.: Terrestrial ecosystem carbon dynamics and climate feedbacks, Nature, 451, 289–292, 2008.

Holmes, R. L.: Computer-assisted quality control in tree-ring dating and measurement, Tree-Ring Bullet., 43, 69–78, 1983.

Houghton, R.: Interannual variability in the global carbon cycle, J. Geophys. Res.-Atmos., 105, 20121–20130, 2000.

Houghton, R., Hackler, J., and Lawrence, K.: The US carbon budget: contributions from land-use change, Science, 285, 574–578, 1999.

Hu, J., Moore, D. J. P., Burns, S. P., and Monson, R. K.: Longer growing seasons lead to less carbon sequestration by a subalpine forest, Glob. Change Biol., 16, 771–783, 2010.

Huxman, T. E., Snyder, K. A., Tissue, D., Leffler, A. J., Ogle, K., Pockman, W. T., Sandquist, D. R., Potts, D. L., and Schwinning, S.: Precipitation pulses and carbon fluxes in semiarid and arid ecosystems, Oecologia, 141, 254–268, 2004.

IPCC: Managing the risks of extreme events and disasters to advance climate change adaptation. A special report of working groups I and II of the Intergovernmental Panel on Climate Change, Cambridge University Press, Cambridge, UK and New York, NY, USA, 2012.

Jeong, S. J., Ho, C. H., Kim, B. M., Feng, S., and Medvigy, D.: Non-linear response of vegetation to coherent warming over northern high latitudes, Remote Sens. Lett., 4, 123–130, 2013.

Jolly, W. M., Dobbertin, M., Zimmermann, N. E., and Reichstein, M.: Divergent vegetation growth responses to the 2003 heat wave in the Swiss Alps, Geophys. Res. Lett., 32, L18409, doi:10.1029/2005GL023252., 2005.

Jongen, M., Pereira, J. S., Aires, L. M. I., and Pio, C. A.: The effects of drought and timing of precipitation on the inter-annual variation in ecosystem-atmosphere exchange in a Mediterranean grassland, Agr. Forest Meteorol., 151, 595–606, 2011.

Jung, M., Reichstein, M., Margolis, H. A., Cescatti, A., Richardson, A. D., Arain, M. A., Arneth, A., Bernhofer, C., Bonal, D., and Chen, J.: Global patterns of land-atmosphere fluxes of carbon dioxide, latent heat, and sensible heat derived from eddy covariance, satellite, and meteorological observations, J. Geophys. Res.-Biogeo., 116, G00J07, doi:10.1029/2010JG001566, 2011.

Jungclaus, J. H., Lorenz, S. J., Timmreck, C., Reick, C. H., Brovkin, V., Six, K., Segschneider, J., Giorgetta, M. A., Crowley, T. J., Pongratz, J., Krivova, N. A., Vieira, L. E., Solanki, S. K., Klocke, D., Botzet, M., Esch, M., Gayler, V., Haak, H., Raddatz, T. J., Roeckner, E., Schnur, R., Widmann, H., Claussen, M., Stevens, B., and Marotzke, J.: Climate and carbon-cycle variability over the last millennium, Clim. Past, 6, 723–737, doi:10.5194/cp-6-723-2010, 2010.

Kaplan, J. O., Krumhardt, K. M., and Zimmermann, N. E.: The effects of land use and climate change on the carbon cycle of Europe over the past 500 years, Glob. Change Biol., 18, 902–914, 2012.

Keenan, T. F., Baker, I., Barr, A., Ciais, P., Davis, K., Dietze, M., Dragoni, D., Gough, C. M., Grant, R., Hollinger, D., Hufkens, K., Poulter, B., McCaughey, H., Raczka, B., Ryu, Y., Schaefer, K., Tian, H., Verbeeck, H., Zhao, M., and Richardson, A. D.: Terrestrial biosphere model performance for inter-annual variability of land-atmosphere $CO_2$ exchange, Glob. Change Biol., 18, 1971–1987, 2012.

Kjellström, E., Nikulin, G., Hansson, U., Strandberg, G., and Ullerstig, A.: 21st century changes in the European climate: uncertainties derived from an ensemble of regional climate model simulations, Tellus A, 63, 24–40, 2011.

Kottek, M., Grieser, J., Beck, C., Rudolf, B., and Rubel, F.: World map of the Koppen–Geiger climate classification updated, Meteorol. Z., 15, 259–264, 2006.

Lei, H. M. and Yang, D. W.: Seasonal and interannual variations in carbon dioxide exchange over a cropland in the North China Plain, Glob. Change Biol., 16, 2944–2957, 2010.

Loveland, T., Reed, B., Brown, J., Ohlen, D., Zhu, Z., Yang, L., and Merchant, J.: Development of a global land cover characteristics database and IGBP DISCover from 1 km AVHRR data, Int. J. Remote Sens., 21, 1303–1330, 2000.

Maignan, F., Bréon, F.-M., Bacour, C., Demarty, J., and Poirson, A.: Interannual vegetation phenology estimates from global AVHRR measurements: comparison with in situ data and applications, Remote Sens. Environ., 112, 496–505, 2008.

Meehl, G. A. and Tebaldi, C.: More intense, more frequent, and longer lasting heat waves in the 21st century, Science, 305, 994–997, 2004.

Moors, E. J., Jacobs, C., Jans, W., Supit, I., Kutsch, W. L., Bernhofer, C., Béziat, P., Buchmann, N., Carrara, A., and Ceschia, E.: Variability in carbon exchange of European croplands, Agr. Ecosyst. Environ., 139, 325–335, 2010.

Moser, L., Fonti, P., Büntgen, U., Esper, J., Luterbacher, J., Franzen, J., and Frank, D.: Timing and duration of European larch growing season along altitudinal gradients in the Swiss Alps, Tree Physiol., 30, 225–233, 2010.

Myneni, R. B., Keeling, C., Tucker, C., Asrar, G., and Nemani, R.: Increased plant growth in the northern high latitudes from 1981 to 1991, Nature, 386, 698–702, 1997.

Nemani, R. R., Keeling, C. D., Hashimoto, H., Jolly, W. M., Piper, S. C., Tucker, C. J., Myneni, R. B., and Running, S. W.: Climate-driven increases in global terrestrial net primary production from 1982 to 1999, Science, 300, 1560–1563, 2003.

Peng, S. S., Piao, S. L., Ciais, P., Myneni, R. B., Chen, A., Chevallier, F., Dolman, A. J., Janssens, I. A., Peñuelas, J., and Zhang, G. : Asymmetric effects of daytime and night-time warming on Northern Hemisphere vegetation, Nature, 501, 88–92, 2013.

Reichstein, M., Ciais, P., Papale, D., Valentini, R., Running, S., Viovy, N., Cramer, W., Granier, A., Ogee, J., Allard, V., Aubinet, M., Bernhofer, C., Buchmann, N., Carrara, A., Grünwald, T., Heimann, M., Heinesch, B., Knohl, A., Kutsch, W., Loustau, D., Manca, G., Matteucci, G., Miglietta, F., Ourcival, J. M., Pilegaard, K., Pumpanen, J., Rambal, S., Schaphoff, S., Seufert, G., Soussana, J. F., Sanz, M. J., Vesala, T., and Zhao, M.: Reduction of ecosystem productivity and respiration during the European summer 2003 climate anomaly: a joint flux tower, remote sensing and modelling analysis, Glob. Change Biol., 13, 634–651, 2007.

Richardson, A. D., Black, T. A., Ciais, P., Delbart, N., Friedl, M. A., Gobron, N., Hollinger, D. Y., Kutsch, W. L., Longdoz, B., and Luyssaert, S.: Influence of spring and autumn phenological transitions on forest ecosystem productivity, Philos. T. R. Soc. B, 365, 3227–3246, 2010.

Rivier, L., Peylin, P., Ciais, P., Gloor, M., Rodenbeck, C., Geels, C., Karstens, U., Bousquet, P., Brandt, J., Heimann, M., and Aerocarb, E.: European $CO_2$ fluxes from atmospheric inversions using regional and global transport models, Climatic Change, 103, 93–115, 2010.

Sacks, W. J., Deryng, D., Foley, J. A., and Ramankutty, N.: Crop planting dates: an analysis of global patterns, Global. Ecol. Biogeogr., 19, 607–620, 2010.

Schär, C., Vidale, P. L., Lüthi, D., Frei, C., Häberli, C., Liniger, M. A., and Appenzeller, C.: The role of increasing temperature variability in European summer heatwaves, Nature, 427, 332–336, 2004.





BGD
10, 17511–17547, 2013

Schimel, D. S., House, J. I., Hibbard, K. A., Bousquet, P., Ciais, P., Peylin, P., Braswell, B. H., Apps, M. J., Baker, D., Bondeau, A., Canadell, J., Churkina, G., Cramer, W., Denning, A. S., Field, C. B., Friedlingstein, P., Goodale, C., Heimann, M., Houghton, R. A., Melillo, J. M., Moore, B., Murdiyarso, D., Noble, I., Pacala, S. W., Prentice, I. C., Raupach, M. R., Rayner, P. J., Scholes, R. J., Steffen, W. L., and Wirth, C.: Recent patterns and mechanisms of carbon exchange by terrestrial ecosystems, Nature, 414, 169–172, 2001.

Schuur, E. A., Vogel, J. G., Crummer, K. G., Lee, H., Sickman, J. O., and Osterkamp, T. E.: The effect of permafrost thaw on old carbon release and net carbon exchange from tundra, Nature, 459, 556–559, 2009.

Schwalm, C. R., Williams, C. A., Schaefer, K., Arneth, A., Bonal, D., Buchmann, N., Chen, J., Law, B. E., Lindroth, A., and Luyssaert, S. : Assimilation exceeds respiration sensitivity to drought: a FLUXNET synthesis, Glob. Change Biol., 16, 657–670, 2010.

Seneviratne, S. I., Lüthi, D., Litschi, M., and Schär, C.: Land–atmosphere coupling and climate change in Europe, Nature, 443, 205–209, 2006.

Stokes, M. A. and Smiley, T. L.: Introduction to tree-ring dating, University of Chicago Press, Chicago, IL, USA, 1968.

Suyker, A. E., Verma, S. B., and Burba, G. G.: Interannual variability in net $CO_2$ exchange of a native tallgrass prairie, Glob. Change Biol., 9, 255–265, 2003.

Tabor, K. and Williams, J. W.: Globally downscaled climate projections for assessing the conservation impacts of climate change, Ecol. Appl., 20, 554–565, 2010.

Tian, H., Melillo, J. M., Kicklighter, D. W., Mcguire, A. D., Helfrich, J. V. K., Moore, B., and Vorosmarty, C. J.: Effect of interannual climate variability on carbon storage in Amazonian ecosystems, Nature, 396, 664–667, 1998.

Tucker, C. J., Pinzon, J. E., Brown, M. E., Slayback, D. A., Pak, E. W., Mahoney, R., Vermote, E. F., and El Saleous, N.: An extended AVHRR 8-km NDVI dataset compatible with MODIS and SPOT vegetation NDVI data, Int. J. Remote Sens., 26, 4485–4498, 2005.

Wigley, T. M. L., Briffa, K. R., and Jones, P. D.: On the average value of correlated time series, with applications in dendroclimatology and hydrometeorology, J. Clim. Appl. Meteorol., 23, 201–213, 1984.

Williams, A. P., Allen, C. D., Macalady, A. K., Griffin, D., Woodhouse, C. A., Meko, D. M., Swetnam, T. W., Rauscher, S. A., Seager, R., and Grissino-Mayer, H. D.: Temperature as a potent driver of regional forest drought stress and tree mortality, Nat. Clim. Change, 3, 292–297, 2013.

Wu, C., Chen, J. M., Black, T. A., Price, D. T., Kurz, W. A., Desai, A. R., Gonsamo, A., Jassal, R. S., Gough, C. M., Bohrer, G., Dragoni, D., Herbst, M., Gielen, B., Berninger, F., Vesala, T., Mammarella, I., Pilegaard, K., and Blanken, P. D.: Interannual variability of net ecosystem productivity in forests is explained by carbon flux phenology in autumn, Global. Ecol. Biogeogr., 22, 994–1006, 2013.

Yuan, W., Luo, Y., Richardson, A. D., Oren, R., Luyssaert, S., Janssens, I. A., Ceulemans, R., Zhou, X., Grünwald, T., and Aubinet, M.: Latitudinal patterns of magnitude and interannual variability in net ecosystem exchange regulated by biological and environmental variables, Glob. Change Biol., 15, 2905–2920, 2009.

Yue, S., Pilon, P., Phinney, B., and Cavadias, G.: The influence of autocorrelation on the ability to detect trend in hydrological series, Hydrol. Process., 16, 1807–1829, 2002.

Zaehle, S., Friend, A. D., Friedlingstein, P., Dentener, F., Peylin, P., and Schulz, M: Carbon and nitrogen cycle dynamics in the O-CN land surface model: 2. Role of the nitrogen cycle in the historical terrestrial carbon balance, Global, Biogeochem. Cy., 24, GB1006, doi:10.1029/2009GB003522, 2010.

Zhang, X., Friedl, M. A., and Schaaf, C.B.: Global vegetation phenology from Moderate Resolution Imaging Spectroradiometer (MODIS): evaluation of global patterns and comparison with in situ measurements, J. Geophys. Res.-Biogeo., 111, G04017, doi:10.1029/2006JG000217, 2006.

Zhao, M. S. and Running, S. W.: Drought-induced reduction in global terrestrial net primary production from 2000 through 2009, Science, 329, 940–943, 2010.

Zhou, L., Tucker, C. J., Kaufmann, R. K., Slayback, D., Shabanov, N. V., and Myneni, R. B.: Variations in northern vegetation activity inferred from satellite data of vegetation index during 1981 to 1999, J. Geophys. Res.-Atmos., 106, 20069–20083, 2001.

**Table 1.** Generalized linear model analyses for the relationships between productivity proxies and climate in different climate zones.

| Carbon proxies[a] | Climate zones[b] | GLM coefficients[c] | | | | Explained variance (%) | | | |
|---|---|---|---|---|---|---|---|---|---|
| | | TEM | WAI | CFD[d] | MMT | TEM | WAI | CFD | MMT |
| Barley yield | Cf | **0.328** | **0.513** | −0.39 | **−0.726** | 0.00 | **11.65** | 0.69 | 2.32 |
| | Cs | 0.905 | **0.426** | 0.01 | **−2.473** | 0.80 | **25.00** | 0.03 | **7.22** |
| | Df | −0.251 | **0.514** | −415.94 | **−0.743** | **1.68** | **7.52** | **16.55** | 2.39 |
| Wheat yield | Cf | 0.176 | **0.593** | −0.51 | **−0.696** | 0.10 | **12.45** | 0.96 | **1.64** |
| | Cs | −0.259 | **0.401** | 0.51 | **−1.993** | **4.69** | **24.98** | 0.01 | **5.75** |
| | Df | **−1.104** | **0.324** | −388.36 | **−0.532** | **11.43** | 1.84 | **12.40** | 1.03 |
| Grain maize yield | Cf | **2.667** | **0.786** | −0.01 | **1.468** | **3.05** | **13.69** | 0.01 | 3.47 |
| | Cs | −1.245 | −0.011 | 1.88 | **−1.626** | 1.18 | 0.00 | 1.18 | **4.79** |
| | Df | **2.712** | **0.481** | 5.31 | **0.609** | 1.41 | **6.44** | 0.00 | 2.08 |
| Potato yield | Cf | **1.372** | **0.156** | −0.02 | 0.436 | **9.24** | **4.01** | 0.04 | **2.26** |
| | Cs | −0.842 | **0.118** | 0.83 | **−0.665** | **8.34** | 2.14 | 1.43 | **5.03** |
| | Df | −0.282 | −0.016 | −1.03 | **−0.264** | 0.61 | 0.11 | 0.15 | 1.94 |
| $NDVI_{gs}$ | Cf | 0.067 | **0.160** | −0.02 | 0.015 | 0.01 | **1.72** | 0.01 | 0.00 |
| | Cs | **−3.813** | **0.464** | −0.05 | 0.095 | **4.03** | **20.25** | 0.04 | 0.01 |
| | Df | **0.181** | 0.001 | 0.00 | −0.040 | **5.22** | 0.00 | 0.02 | 0.75 |
| $GPP_{gs}$ | Cf | 0.081 | **0.497** | 0.14 | −0.166 | 0.48 | **27.41** | 0.76 | 0.16 |
| | Cs | **−2.125** | **0.892** | −0.01 | **−3.726** | 0.14 | **24.18** | 0.01 | **18.93** |
| | Df | 0.124 | **0.169** | 0.33 | **−0.086** | 0.78 | **13.14** | 0.33 | 0.89 |
| $FAPAR_{gs}$ | Cf | **−0.266** | **0.299** | 0.05 | 0.146 | **2.26** | **20.16** | 0.25 | 0.32 |
| | Cs | **−1.811** | **0.466** | −0.01 | **−2.028** | 0.84 | **23.89** | 0.03 | **18.46** |
| | Df | 0.011 | **0.180** | 0.39 | −0.041 | **4.25** | **22.96** | 0.47 | 0.30 |

Note: Bold values are statistically significant ($p < 0.05$).
[a] NDVIgs, GPPgs and FAPARgs are accumulated growing season (March–September) NDVI, GPP and FAPAR, respectively. All carbon proxies are detrended by fitting a cubic smoothing spline (in detail see Sect. 2.2).
[b] Climate zones used in this study are based on the Köppen–Geiger climate classification.
[c] GLM: generalized linear model. TEM, WAI, CFD, MMT are mean growing season temperature, total growing season water availability index, total spring (March–May) consecutive frost days and mean growing season maximum of daily maximum temperature. Growing seasons are different for different crops. We fixed the growing season as March–June for barley and wheat and as March–September for potato and grain maize.
[d] The scaling factor for the GLM coefficients of CFD is $10^{-3}$.





BGD
10, 17511–17547, 2013

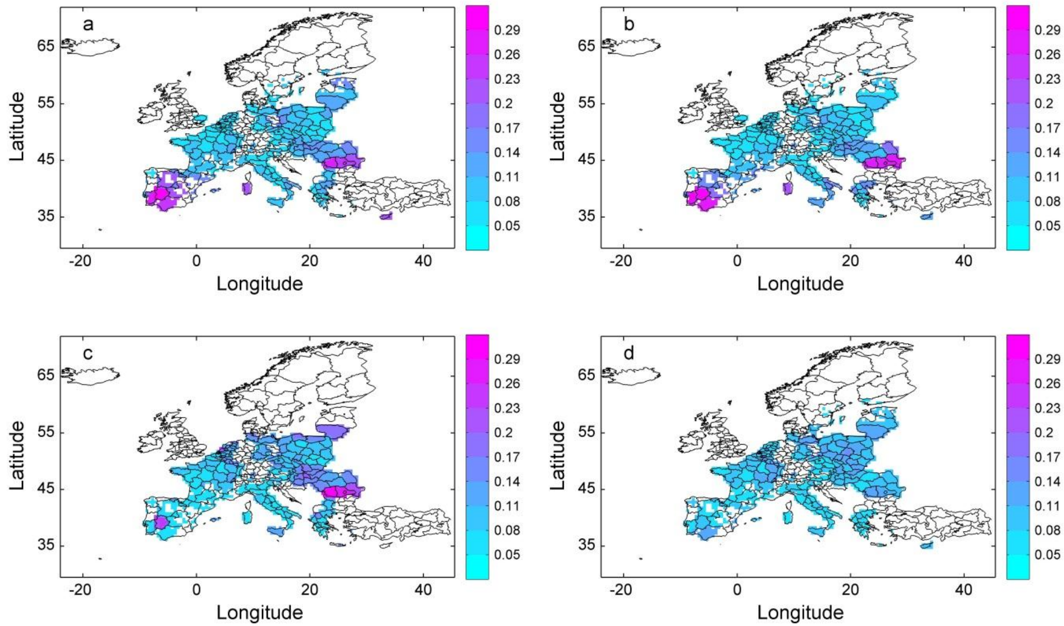


**Fig. 1.** Spatial patterns of the coefficients of variation (CV) of crop yield data. Spatial patterns of CV of detrended crop yield data during 1975–2009 for barley **(a)**, wheat **(b)**, grain maize **(c)** and potatoes **(d)**. Blank region indicates that there is no crop yield records or with very low (< 5 %) fraction of croplands in those pixels.





BGD
10, 17511–17547, 2013

Climate-mediated variability in the terrestrial productivity

X. Wu et al.

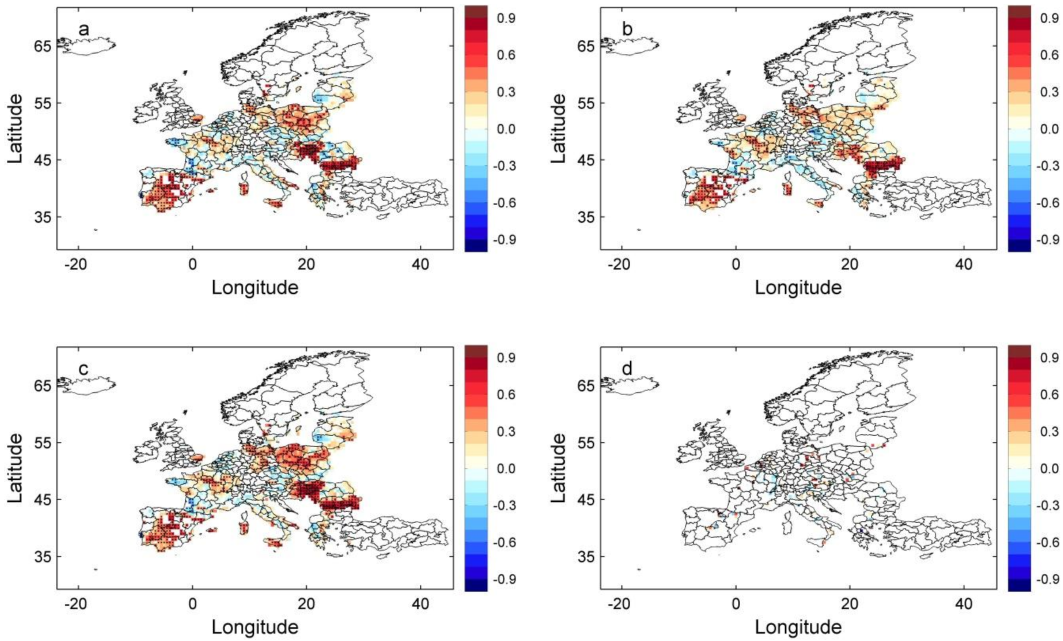


**Fig. 2.** Spatial patterns of correlation coefficients between barley yield and others proxies. Spatial distribution of Spearman correlation coefficients between the IAV of barley yield and IAV of correspondingly growing season (March–June for barley) summed NDVI **(a)**, GPP **(b)**, and FAPAR **(c)** and standard tree ring index **(d)**. Significant relationships were marked by black points. Blank region indicates that there is no crop yield records or with very low (< 5 %) fraction of croplands in those pixels.





BGD
10, 17511–17547, 2013

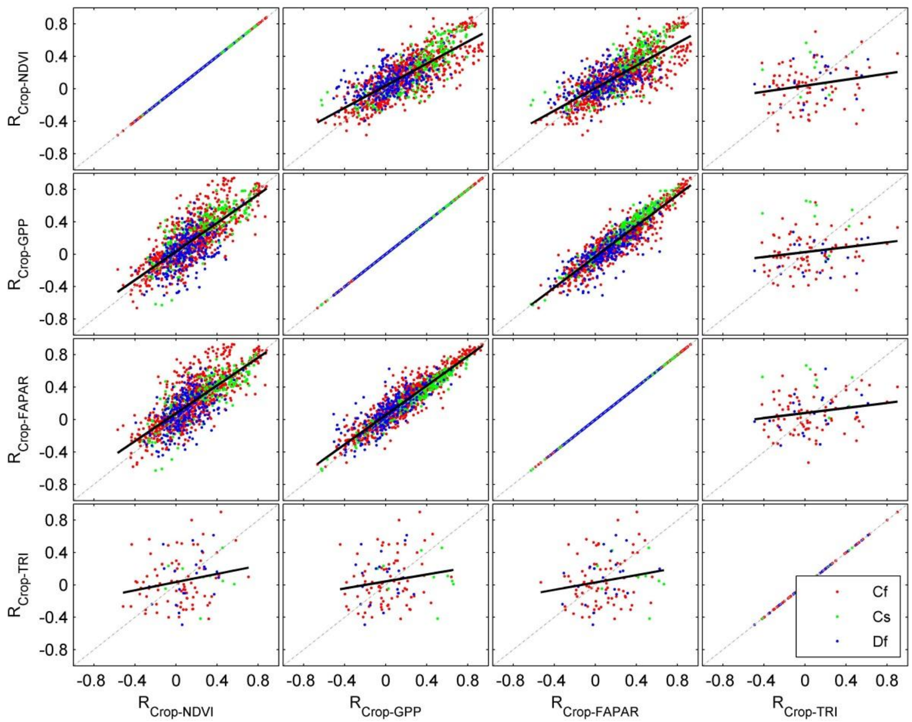


**Fig. 3.** Relationships between barley yield IAV and IAV of others proxies. Scatter plot of the relationships between the correlation coefficients of IAV of barley yield and IAV of growing season (March–June for barley) summed NDVI, GPP, and FAPAR, and standard TRI. Different colors indicate different Köppen–Geiger climate zones.





BGD
10, 17511–17547, 2013

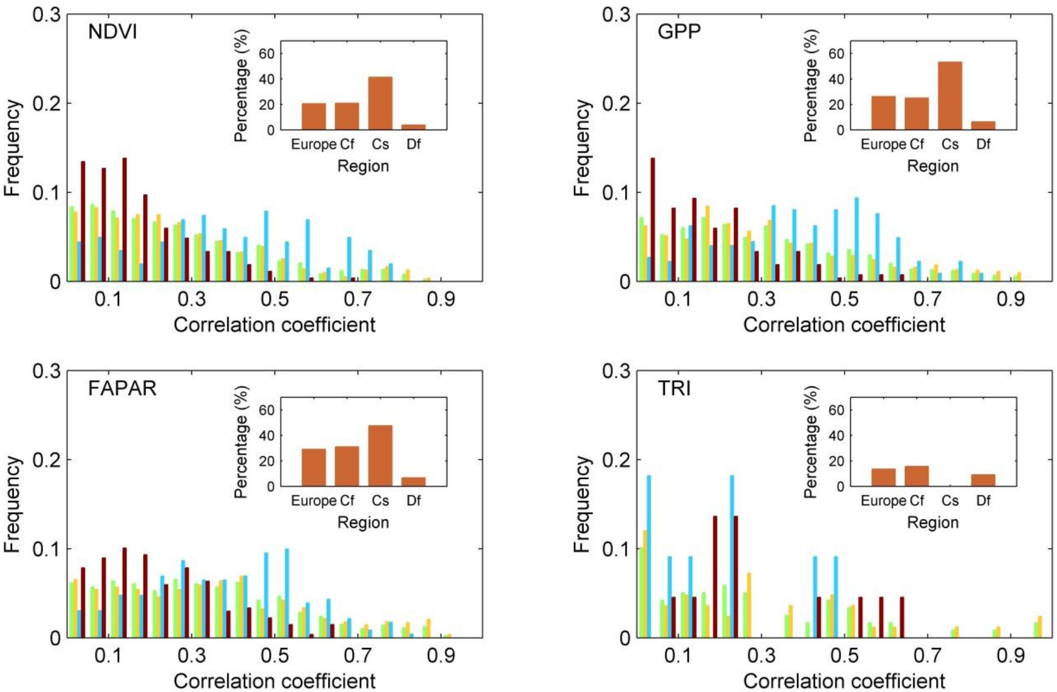


**Fig. 4.** Frequency distributions of correlation coefficients of IAV of barley yield and IAV of growing season (March–June) summed NDVI, GPP, and FAPAR and standard TRI in Europe (green bars) and climate zones: Cf (yellow bars), Cs (light blue bars), and Df (brown bars). Percentage of pixels where there are significant ($p < 0.1$) relationships between IAV of barley yield and IAV of growing season summed NDVI, GPP, and FAPAR and TRI are shown in the inlet figures.





BGD
10, 17511–17547, 2013

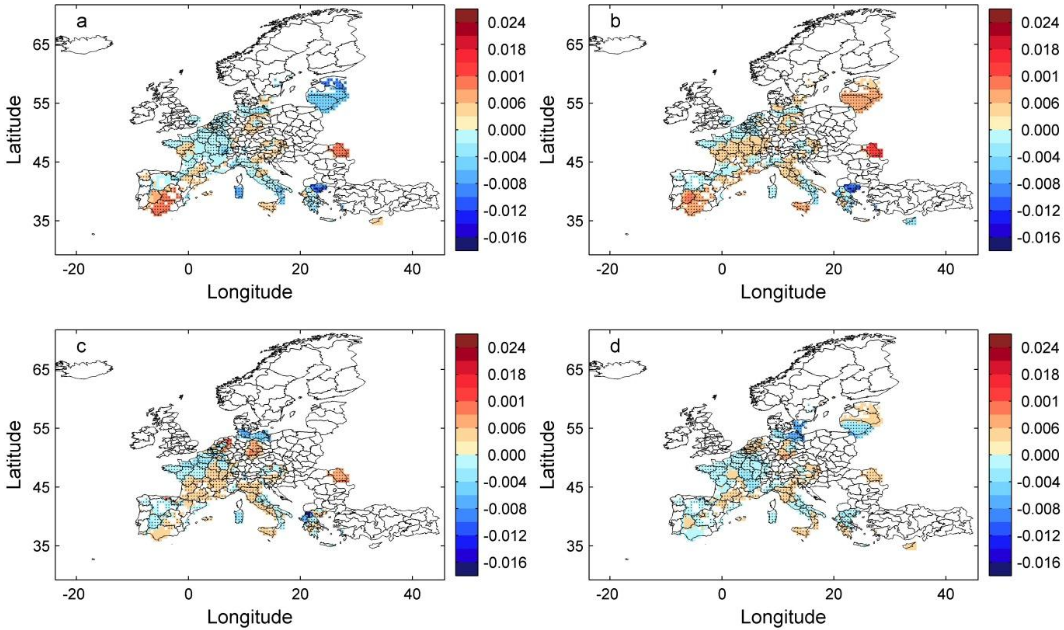


**Fig. 5.** Spatial patterns of the trends in crop yield interannual variability. Spatial patterns of the estimated trends in the moving coefficients of variation (CV) of the detrended crop yield calculated using a 10 yr sliding window with 1 yr lag during 1975–2009 for barley **(a)**, wheat **(b)**, grain maize **(c)** and potatoes **(d)**. The trends in time series are estimated by the Theil–Sen slope method (Yue et al., 2002). Significant trends were marked by black points. Blank region indicates that there is no crop yield records or with very low (< 5 %) fraction of cropland in those pixels.

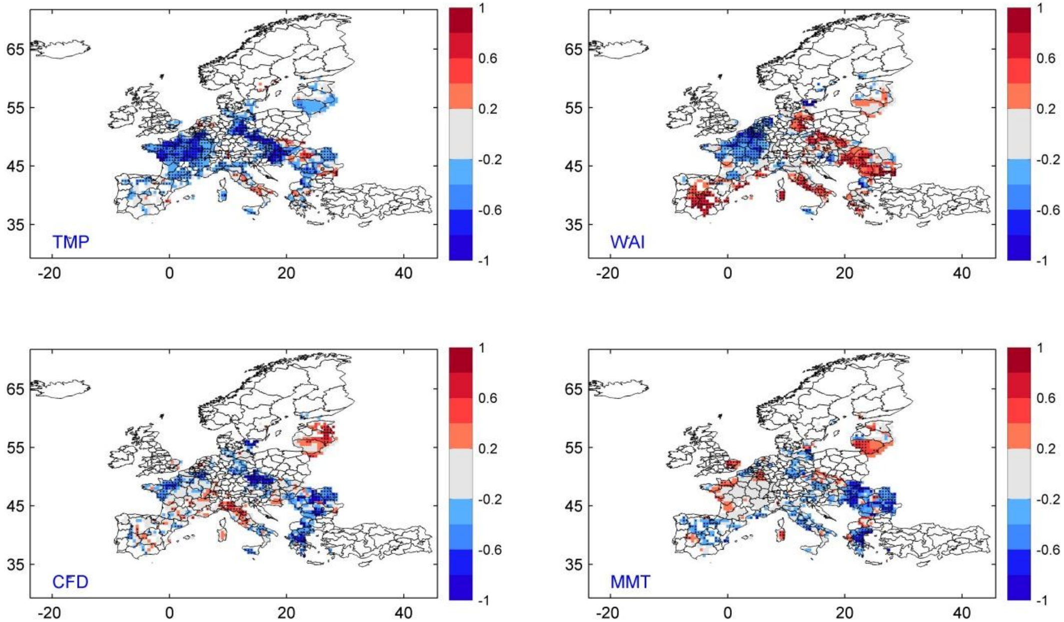


**Fig. 6.** Response function coefficients between barley yield and mean growing season temperature (TMP), total growing season water availability index (WAI) and consecutive frost days (CFD) and mean growing season maximum of daily maximum mean temperature (MMT). Significant response function coefficients between barley yield and climate are marked by black points. Blank regions indicate that there is no crop yield records or with very low (< 5 %) fraction of croplands in those pixels.





BGD
10, 17511–17547, 2013

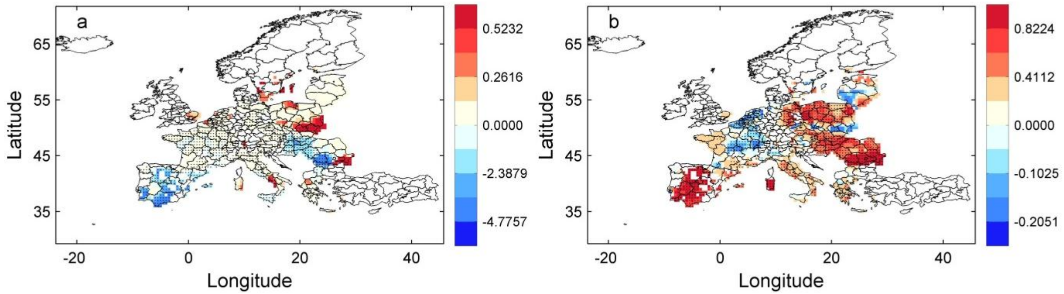


**Fig. 7.** Spatial patterns of the general climate sensitivity of barley yield. Climate sensitivity of barley yield to the mean growing-season temperature **(a)** and total growing season water availability index **(b)** was estimated by the slope of linear regression during 1975–2009. Significant slopes were marked by black points. Blank regions indicate that there is no crop yield records or with very low (< 5 %) fraction of croplands in those pixels.





BGD
10, 17511–17547, 2013

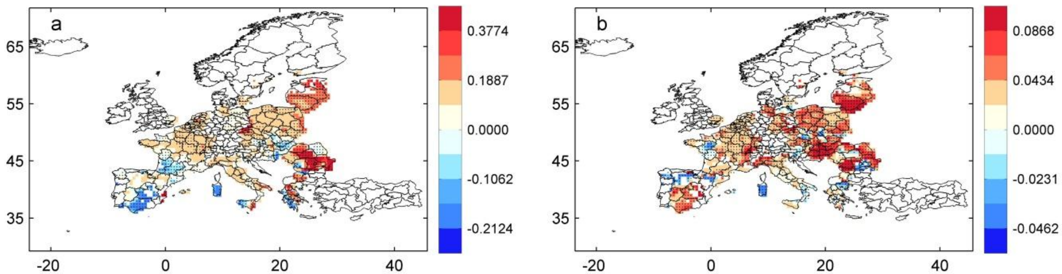


**Fig. 8.** Spatial patterns of the linear trends in moving climate sensitivities of barley yield. The linear trends in moving climate sensitivity of barley yield to the mean growing-season temperature **(a)** and total growing season water availability index **(b)** were estimated by the Theil–Sen slope method using a 10 yr sliding window with 1 yr lag during 1975–2009. Significant trends were marked by black points. Blank regions indicate that there is no crop yield records or with very low (< 5 %) fraction of croplands in those pixels.





BGD
10, 17511–17547, 2013

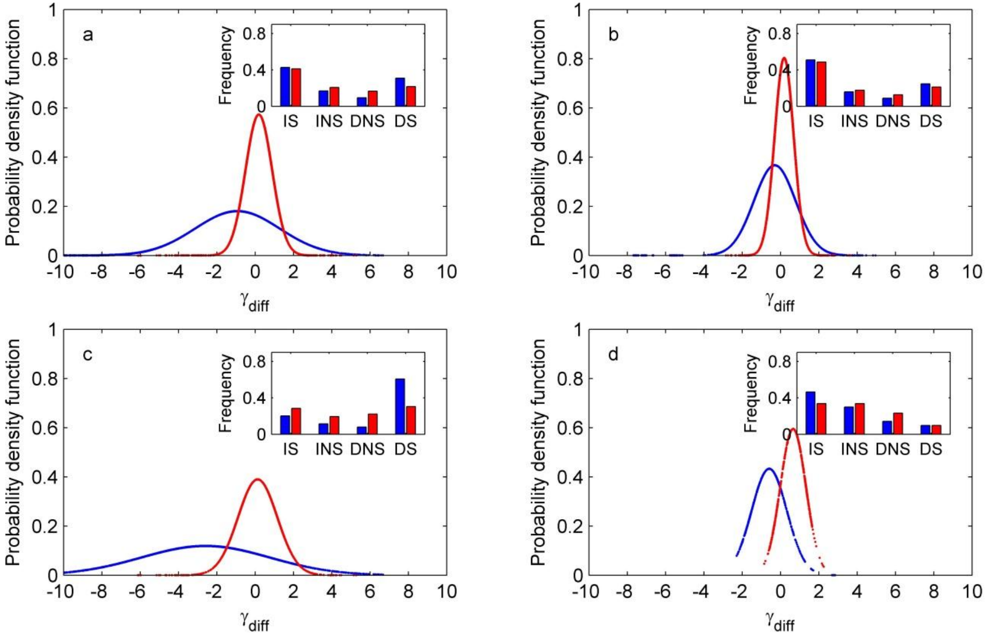


**Fig. 9.** Probability density function for the differences of moving climate sensitivities of barley yield in different climate zones. Probability density function for the differences of moving climate sensitivities of barley yield to mean growing season temperature (blue line) and total growing season water availability index (red line) between 1995–2008 and 1982–1995 for Europe **(a)**, and climate zones Cf **(b)**, Cs **(c)**, and Df **(d)**. The inlet shows the percentages of pixels suffering the four different trend types (significantly increasing, IS; increasing but not significant, INS; decreasing but not significant, DNS; significantly decreasing, DS) for climate sensitivities of barley yield to mean growing season temperature (blue bars) and total growing season water availability index (red bars).





BGD
10, 17511–17547, 2013